Operator Based Multiscale Method for Compressible Flow

H. Zhou, SPE, Stanford U.; **H.A. Tchelepi**, SPE, Stanford U.;

Abstract

Multiscale methods have been developed for accurate and efficient numerical solution of flow problems in large-scale heterogeneous reservoirs. A scalable and extendible Operator Based Multiscale Method (OBMM) is described here. OBMM is cast as a general algebraic framework. It is natural and convenient to incorporate more physics in OBMM for multiscale computation. In OBMM, two operators are constructed: prolongation and restriction. The prolongation operator is constructed by assembling the multiscale basis functions. The specific form of the restriction operator depends on the coarse-scale discretization formulation (e.g., finite-volume or finite-element). The coarse-scale pressure equation is obtained algebraically by applying the prolongation and restriction operators to the fine-scale flow equations. Solving the coarse-scale equation results in a high quality coarse-scale pressure. The fine scale pressure can be reconstructed by applying the prolongation operator to the coarse-scale pressure. A conservative fine-scale velocity field is then reconstructed to solve the transport (saturation) equation. We describe the OBMM approach for multiscale modeling of compressible multiphase flow. We show that extension from incompressible to compressible flows is straightforward. No special treatment for compressibility is required. The efficiency of multiscale formulations over standard fine-scale methods is retained by OBMM. The accuracy of OBMM is demonstrated using several numerical examples including a challenging depletion problem in a strongly heterogeneous permeability field (SPE 10).

Introduction

The accuracy of simulating subsurface flow relies strongly on the detailed geologic description of the porous formation. Formation properties such as porosity and permeability typically vary over many scales. As a result, it is not unusual for a detailed geologic description to require $10^7 - 10^8$ grid cells. However, this level of resolution is far beyond the computational capability of state-of-the-art reservoir simulators (10^6 grid cells). Moreover, in many applications, a large number of reservoir simulations are performed (e.g., history matching, sensitivity analysis and stochastic simulation). Thus, it is necessary to have an efficient and accurate computational method to study these highly detailed models.

Multiscale formulations are very promising due to their ability to resolve fine-scale information accurately without direct solution of the global fine-scale equations. Recently, there has been increasing interest in multiscale methods. Hou and Wu (1997) proposed a multiscale finite-element method (MsFEM) that captures the fine-scale information by constructing special basis functions within each element. However, the reconstructed fine-scale velocity is not conservative. Later, Chen and Hou (2003) proposed a conservative mixed finite-element multiscale method. Another multiscale mixed finite-element method was presented by Arbogast (2002) and Arbogast and Bryant (2002). Numerical Green functions were used to resolve the fine-scale information, which are then coupled with coarse-scale operators to obtain the global solution. Aarnes (2004) proposed a modified mixed finite-element method, which constructs special basis functions sensitive to the nature of the elliptic problem. Chen *et al.* (2003) developed a local-global upscaling method by extracting local boundary conditions from a global solution, and then constructing coarse scale system from local solutions. All these methods considered incompressible flow in heterogeneous porous media where the pressure equation is elliptic.

A multiscale finite-volume method (MsFVM) was proposed by Jenny, Lee and Tchelepi (2003, 2004, 2006) for heterogeneous elliptic problems. They employed two sets of basis functions — dual and primal. The dual basis functions are identical to those of Hou and Wu (1997), while the primal basis functions are obtained by solving local elliptic problems with Neumann boundary conditions calculated from the dual basis functions.

Existing multiscale methods (Aarnes 2004; Arbogast 2002; Chen and Hou 2003; Hou and Wu 1997; Jenny, Lee, and Tchelepi 2003) deal with the incompressible flow problem only. However, compressibility will be significant if a gas phase is present. Gas has a large compressibility, which is a strong function of pressure. Therefore, there can be significant spatial compressibility variations in the reservoir, and this is a challenge for multiscale modeling. Very recently, Lunati and Jenny (2005) considered compressible multiphase flow in the framework of MsFVM. They proposed three models to account for the effects of compressibility. Using those models, compressibility effects were represented in the coarse-scale equations and the reconstructed fine-scale fluxes according to the magnitude of compressibility.

Motivated to construct a flexible algebraic multiscale framework that can deal with compressible multiphase flow in highly detailed heterogeneous models, we developed an operator based multiscale method (OBMM). The OBMM algorithm is composed of four steps: (1) constructing the prolongation and restriction operators, (2) assembling and solving the coarse-scale pressure equations, (3) reconstructing the fine-scale pressure and velocity fields, and (4) solving the fine-scale transport equations.

OBMM is a general algebraic multiscale framework for compressible multiphase flow. This algebraic framework can also be extended naturally from structured to unstructured grid. Moreover, the OBMM approach may be used to employ multiscale solution strategies in existing simulators with a relatively small investment.

Operator Based Multiscale Method

In this section, we describe the operator based multiscale method (OBMM) for the two-phase flow problem. We show that for incompressible flow, OBMM is identical to the original MsFVM(Jenny, Lee, and Tchelepi 2003). The effects of compressibility are taken into account naturally when constructing the coarse-scale operators. The basis functions and reconstructed fine-scale fluxes also account for the compressibility effects. The overall algorithm to solve coupled flow and transport problems with the OBMM framework is described, and adaptive computation of the basis functions is discussed.

Model Equations.. We consider immiscible two-phase flow in porous media. Extension to three-phase flow is straightforward. Gravity and capillarity are neglected here. The governing equations are the mass conservation equations of the two phases,

$$\begin{aligned} &\frac{\partial(\phi b_l)}{\partial t} + \nabla \cdot (b_l u_l) = q_l, \\ &u_l = -\lambda_l \nabla p, \\ &\lambda_l = \frac{k k_{rl}}{\mu}, \end{aligned} \qquad \ldots\ldots\ldots\ldots\ldots\ldots\ldots \quad (1)$$

where $l = 1,2$ denotes the two phases; b_l is the inverse of the phase formation-volume factor, which is defined as the ratio of density at reservoir conditions to density at standard conditions; u_l is the

This paper (SPE 106254) was revised for publication from paper SPE 106254, presented at the 2007 SPE Reservoir Simulation Symposium held in The Woodlands, Texas, U.S.A., 26-28 February 2007. Original manuscript received for review December 14, 2006. Revised manuscript received November 15, 2007. Manuscript peer approved December 1, 2007.

phase volumetric flux at reservoir conditions; q_l is the source term; λ_l is the phase mobility; k_{rl} is the phase relative permeability; ϕ and k are the porosity and absolute permeability.

Because multiscale methods are usually applied only to the pressure equation, the flow (pressure and total velocity) and transport problems are treated separately and differently. Thus, the flow and transport equations are solved sequentially using either an IMPES (Implicit Pressure Explicit Saturation) or a sequential fully implicit (SFI) Method (Tchelepi *et al.* (2007)). Here we adopt the sequential fully implicit approach. The linearized discrete pressure equation can be obtained from Eq.1 through simple algebraic manipulation. The semi-discrete equation for iteration $\nu+1$ at time step $n+1$ is

$$\begin{aligned} C\frac{p^{\nu+1}-p^{\nu}}{\Delta t} &- \alpha_1^{\nu}\nabla\cdot\left(b_1^{\nu}\lambda_1^{\nu}\nabla p^{\nu+1}\right) \\ &- \alpha_2^{\nu}\nabla\cdot\left(b_2^{\nu}\lambda_2^{\nu}\nabla p^{\nu+1}\right) \\ = RHS, & \end{aligned} \quad \ldots\ldots\ldots\ldots (2)$$

where,

$$\begin{aligned} \alpha_1^{\nu} &= 1/b_1^{\nu}, \\ \alpha_2^{\nu} &= 1/b_2^{\nu}, \\ C &= \left(\frac{\partial\phi}{\partial p}-\phi^n(b_1^nS_1^n\frac{\partial\alpha_1}{\partial p}+b_2^nS_2^n\frac{\partial\alpha_2}{\partial p})\right. \\ &\quad \left.+\Delta t\frac{\partial(\alpha_1q_1+\alpha_2q_2)}{\partial p}\right)^{\nu}, \qquad \ldots\ldots (3) \\ RHS &= -\frac{\phi^{\nu}}{\Delta t}+\frac{\phi^n}{\Delta t}\left(\alpha_1^{\nu}b_1^nS_1^n+\alpha_2^{\nu}b_2^nS_2^n\right) \\ &\quad -(\alpha_1q_1^{\nu}+\alpha_2q_2^{\nu}). \end{aligned}$$

Given a fine-scale problem, Eq.2 can be written in matrix form as

$$(\mathbf{T}_f-\mathbf{C}_f)\mathbf{p}_f=\mathbf{r}_f, \quad \ldots\ldots\ldots\ldots\ldots\ldots\ldots (4)$$

where $\mathbf{T}_f$ is the fine-scale transmissibility matrix associated with the flow part, $\mathbf{C}_f$ is the fine-scale compressibility matrix associated with the accumulation part, $\mathbf{p}_f$ denotes the fine-scale pressure vector, and $\mathbf{r}_f$ is the fine-scale right-hand-side vector.

The linearized discrete form of the transport equation for phase 1 is

$$\begin{aligned} &\frac{\phi^{\nu+1}b_1^{\nu+1}S_1^{\nu+1}-\phi^nb_1^nS_1^n}{\Delta t} \\ &=\nabla\cdot\left\{b_1^{\nu+1}\left[f_1^{\nu}+\left.\frac{\partial f_1}{\partial S_1}\right|^{\nu}(S_1^{\nu+1}-S_1^{\nu})\right]\mathbf{u}_T^{\nu+1}\right\}-q_1, \end{aligned} \quad (5)$$

where f_1 is the fractional flow of phase 1, and $\mathbf{u}_T$ is the total velocity.

Prolongation Operator.. The multiscale prolongation operator, $\mathcal{P}$, is defined as the mapping from coarse-scale pressure to fine-scale pressure, i.e.,

$$\mathbf{p}_f=\mathcal{P}\mathbf{p}_c, \quad \ldots\ldots\ldots\ldots\ldots\ldots\ldots\ldots (6)$$

where $\mathbf{p}_c$ denotes the cell-center coarse-scale pressure. Hou and Wu (1997) used a set of specially constructed basis functions to relate the fine and coarse pressures. Although their study was for the incompressible flow (elliptic) problem, we have found that their basis functions also work for parabolic problems (e.g., compressible flow). The construction of the basis functions for Eq.1 is discussed below.

Considering a two dimensional multiscale grid as shown in Fig.1, the physical domain is partitioned into disjoint primal coarse blocks, and each coarse block is further partitioned into fine cells. Dual coarse blocks are defined by connecting the centers of primal coarse blocks. The idea of the dual coarse grid is an alternative to the oversampling approach proposed by Hou and Wu (1997). As shown by Hou and Wu (1997), oversampling is necessary to reduce the error caused by the imposed reduced local boundary conditions. The dual coarse grid offers significant advantages. It ensures a locally

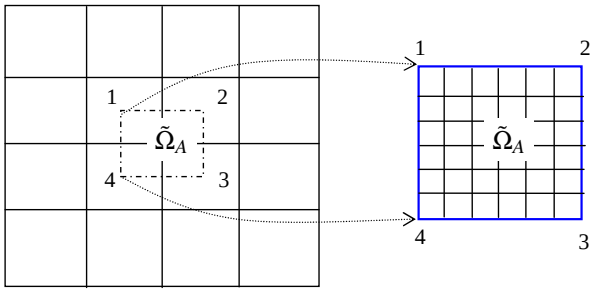

Fig. 1—Two-dimensional multiscale grid with a typical dual control volume. The enlarged dual control volume shows the underlying fine grid.

conservative operator on the coarse grid by extracting fluxes across the primal coarse blocks. Such fluxes are located near the centers of the respective dual blocks; as a result, the influence of the imposed local boundary condition is small.

Following the idea of the reduced boundary condition in Hou and Wu (1997), a basis function associated with coarse node i ($i=1,\ldots,4$) in dual block $\tilde{\Omega}_A$ is obtained by solving the elliptic part of Eq.1,

$$\begin{aligned} &\alpha_1^{\nu}\nabla\cdot\left(b_1^{\nu}\lambda_1^{\nu}\nabla\phi_A^i\right)+\alpha_2^{\nu}\nabla\cdot\left(b_2^{\nu}\lambda_2^{\nu}\nabla\phi_A^i\right)=0 \ \text{ in } \tilde{\Omega}_A, \\ &\alpha_1^{\nu}\frac{\partial}{\partial x_t}\left(b_1^{\nu}\lambda_1^{\nu}\frac{\partial\phi_A^i}{\partial x_t}\right)+\alpha_2^{\nu}\frac{\partial}{\partial x_t}\left(b_2^{\nu}\lambda_2^{\nu}\frac{\partial\phi_A^i}{\partial x_t}\right)=0 \ \text{ on } \partial\tilde{\Omega}_A, \\ &\phi_A^i(\mathbf{x}_j)=\delta_{ij}, \end{aligned} \quad (7)$$

where subscript t denotes the component tangential to the boundary, and j denotes any coarse node in $\tilde{\Omega}_A$ ($j=1,\ldots,4$). Note that the inverse of formation volume factors (b_l) are included in Eq.7 to account for the local effects of compressibility on the basis functions. Some other boundary conditions for the basis functions are also possible, e.g., constant pressure boundary, uniform flux boundary, etc. The reduced boundary condition has been shown to yield quite accurate results in isotropic, highly heterogeneous problems (Hou and Wu 1997; Jenny, Lee, and Tchelepi 2003). Moreover, as will be clear from the following discussion, the construction of OBMM is actually independent of the specific form of the basis functions. Any appropriate basis function can be employed in our framework.

With the basis functions, we can easily construct the prolongation operator. Let K be the global index of a coarse node, $i_{K,A}$ be the local index of node K in dual block $\tilde{\Omega}_A$, and $\mathcal{D}_K$ the set of dual blocks intersected by node K. For Cartesian grid, the number of elements in $\mathcal{D}_K$ is 2^d, where d is the number of dimensions. Using a global point of view, a basis function can be written as

$$\phi_K=\sum_{\tilde{\Omega}_A\in\mathcal{D}_K}\phi_A^{i_{K,A}}. \quad \ldots\ldots\ldots\ldots\ldots\ldots\ldots (8)$$

The multiscale prolongation operator, $\mathcal{P}$, is an $n\times N$ matrix, where n is the number of global fine nodes and N is the number of global coarse nodes. Let k denote a fine node and K a coarse node. Then one has

$$\mathcal{P}_{k,K}=\phi_K(\boldsymbol{x}_k) \quad \ldots\ldots\ldots\ldots\ldots\ldots\ldots\ldots (9)$$

Restriction Operator.. Plugging Eq.6 into Eq.4, one obtains

$$(\mathbf{T}_f-\mathbf{C}_f)\mathcal{P}\mathbf{p}_c=\mathbf{r}_f. \quad \ldots\ldots\ldots\ldots\ldots\ldots\ldots (10)$$

The significance of Eq.10 is that its unknowns are coarse-scale pressures. We need to apply a restriction operator, $\mathcal{R}$, that provides a mapping from fine to coarse space. We write

$$\mathcal{R}(\mathbf{T}_f-\mathbf{C}_f)\mathcal{P}\mathbf{p}_c=\mathcal{R}\mathbf{r}_f, \quad \ldots\ldots\ldots\ldots\ldots\ldots (11)$$

or

$$(\mathbf{T}_c-\mathbf{C}_c)\mathbf{p}_c=\mathbf{r}_c, \quad \ldots\ldots\ldots\ldots\ldots\ldots\ldots (12)$$

where $\mathbf{T}_c, \mathbf{C}_c, \mathbf{r}_c$ are the coarse-scale counterparts of $\mathbf{T}_f, \mathbf{C}_f, \mathbf{r}_f$, and are defined as

$$\begin{array}{rcl} \mathbf{T}_c & = & \mathcal{R}\mathbf{T}_f\mathcal{P} \\ \mathbf{C}_c & = & \mathcal{R}\mathbf{C}_f\mathcal{P} \\ \mathbf{r}_c & = & \mathcal{R}\mathbf{r}_f. \end{array} \quad \ldots\ldots\ldots\ldots\ldots\ldots\ldots\ldots \quad (13)$$

Eq.12 is the coarse-scale equation we need to solve.

The restriction operator, $\mathcal{R}$, maps the fine-scale discretization equations into the coarse scale; it is not unique. The specific choice for $\mathcal{R}$ depends on the discretization scheme (e.g., finite element, or finite volume). We denote a fine-scale conservation equation by E. A finite volume formulation starts with

$$\int_{\Omega_k} E\,\mathrm{d}V = 0 \quad (\forall \text{ fine cell } \Omega_k, k = 1,\ldots,n). \quad \ldots\ldots\ldots \quad (14)$$

A coarse-scale finite volume formulation requires

$$\int_{\Omega_K} E\,\mathrm{d}V = 0 \quad (\forall \text{ coarse block } \Omega_K, K = 1,\ldots,N). \quad \ldots \quad (15)$$

Comparing Eq.14 and Eq.15, it is clear that Eq.15 can be obtained by summing Eq.14 for all the fine cells inside a coarse block K, i.e.,

$$\int_{\Omega_K} E\,\mathrm{d}V = \sum_{\Omega_k \in \Omega_K} \int_{\Omega_k} E\,\mathrm{d}V. \quad \ldots\ldots\ldots\ldots\ldots\ldots\ldots \quad (16)$$

The summation in Eq.16 can be represented by the restriction operator, $\mathcal{R}$, as follows

$$\mathcal{R}_{K,k} = \begin{cases} 1 & \text{if } \Omega_k \subset \Omega_K \\ 0 & \text{otherwise} \end{cases} \quad (K = 1,\ldots,N; k = 1,\ldots,n). \quad (17)$$

It is also important to note that the restriction operator does not depend on the detailed discretization scheme (i.e., backward difference or central difference, etc.) and thus is general for a given formulation.

In a Galerkin-type finite element method, the coarse-scale equation may be written as

$$\int_{\Omega_K} \phi_M E\,\mathrm{d}V = 0 \quad (K, M = 1,\ldots,N) \quad \ldots\ldots\ldots\ldots\ldots \quad (18)$$

and one can show that $\mathcal{R}$ takes the following form

$$\mathcal{R} = \mathcal{P}^T. \quad \ldots\ldots\ldots\ldots\ldots\ldots\ldots\ldots\ldots\ldots\ldots\ldots \quad (19)$$

Zhou (2006) provides a detailed treatment for finite-element based multiscale formulations.

Coarse-Scale Operators.. Given the prolongation and restriction operators defined above, the coarse-scale system, Eq.12, can be constructed. We shed some light on the physical meaning of the coarse-scale operators. The focus is on OBMM using the finite-volume formulation (i.e., $\mathcal{R}$ given by Eq.17).

To make the analysis easier, consider a one-dimensional problem. Fig.2 shows the grid with coarse blocks $K-1, K, K+1$, and fine cells $k-4,\ldots,k+4$. We first look at the incompressible case where

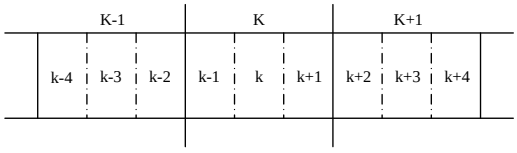

Fig. 2—One-dimensional multiscale grid

Eq.1 becomes

$$\nabla \cdot (\lambda_t \nabla p) = q_t, \quad \ldots\ldots\ldots\ldots\ldots\ldots\ldots\ldots\ldots \quad (20)$$

where, $\lambda_t = \lambda_1 + \lambda_2$ is the total mobility, and q_t is the total source term. Using a central difference scheme in the fine-scale discretization, the OBMM algorithm gives three non-zeros elements for the K^{th} row of the coarse-scale transmissibility matrix, i.e.,

$$\begin{array}{rcl} T_{cK,K-1} & = & -\dfrac{\lambda_{k-3/2}}{\Delta x}\left(\phi_{K-1}(x_{k-1}) - \phi_{K-1}(x_{k-2})\right), \\ T_{cK,K} & = & -\dfrac{\lambda_{k-3/2}}{\Delta x}\left(\phi_K(x_{k-1}) - \phi_K(x_{k-2})\right) \\ & & +\dfrac{\lambda_{k+3/2}}{\Delta x}\left(\phi_K(x_{k+2}) - \phi_{K-1}(x_{k+1})\right), \\ T_{cK,K+1} & = & -\dfrac{\lambda_{k+3/2}}{\Delta x}\left(\phi_{K+1}(x_{k+2}) - \phi_{K+1}(x_{k+1})\right). \end{array} \quad . \quad (21)$$

These coarse-scale operators are exactly the same as the effective coarse-grid transmissibility constructed by Jenny *et al.*. (2003). For example, from Eq.21, $T_{cK,K-1}$ is the flux across the interface between coarse blocks $K-1$ and K with respect to a unit pressure at node $K-1$.

Compressibility is taken into account in the basis functions, Eq.7, and in constructing the coarse-scale transmissibility and compressibility matrices, Eq.13. The fine-scale fluxes represented by $\mathbf{T}_f$ contain compressibility effects, and OBMM gives the coarse-scale fluxes by summing up the fine-scale fluxes in a coarse block. Therefore, the effective transmissibility constructed by OBMM accounts for compressibility of the flow. The coarse-scale compressibility matrix in Eq.13 distribute the accumulation terms in the coarse grid according to the underlying fine-scale accumulation terms. By construction, the scheme is conservative on both the fine and coarse scales.

Compared with the original MsFVM for incompressible problems, OBMM gives exactly the same coarse scale system when using a finite-volume type restriction operator. However, the construction using OBMM is much simpler. Through OBMM, we can easily build the coarse scale system on top of a fine scale formulation by simply providing the restriction and prolongation operators. Therefore, OBMM provides a great advantage in developing multiscale simulators from existing fine-scale codes.

When more physics needs to be included in the MsFVM, special treatment is necessary to formulate the new coarse scale system, which was what Lunati and Jenny (2005) did to extend the original MsFVM to compressible flow. In their discrete formulation, they assumed that the coarse scale accumulation term is diagonal matrix (i.e., the contribution to coarse scale accumulation in a coarse block is only from the block itself), and they proposed three models to compute that contribution. In their most accurate model (FSA, referring to Fine Scale Accumulation), the accumulation part is calculated at the fine scale from the dual pressure. In the MsFVM construction, the dual pressure in one primal coarse block depends on the coarse scale pressure in all of the neighboring coarse blocks. Consequently, to accurately compute the coarse scale accumulation from the fine scale dual pressure, we should have a multi-diagonal matrix (3^d in d-dimensional space) instead of a diagonal one. Lunati and Jenny (2005) imposed additional constraints to get a diagonal accumulation matrix from FSA. In OBMM, on the other hand, there is no assumption on the form of the coarse scale system. If we choose to compute coarse scale accumulation from the fine-scale dual pressure, we naturally obtain a 3^d-diagonal matrix for accumulation, which is the most accurate representation.

In addition, due the difficulty in eliminating saturation in the coarse-scale equations, the derived coarse scale pressure system by Lunati and Jenny (2005) has dependency on saturation, which may introduce some numerical difficulty in multiphase flow problems. In OBMM, one can easily eliminate saturation from the pressure equation on the fine scale, and then the construction of the coarse scale pressure system is independent of saturation, as in Eq.2.

Fine-Scale Velocity.. The coarse-scale pressure, $\mathbf{p}_c$, is obtained from Eq.12, and then the dual fine-scale pressure, $\mathbf{p}_d$, is recon-

```
ν_p = 1; ν_s = 1; p^{ν_p} = p^n; S^{ν_s} = S^n
/* outer loop */
while ( pressure equation not converged)
    calculate fine-scale operators;
    update basis functions;
    assemble prolongation operator;
    calculate coarse-scale operators;
    solve for coarse-scale pressure, p_c;
    reconstruct dual fine-scale pressure, p_d;
    reconstruct primal fine-scale pressure, p_v;
    ν_p = ν_p + 1; p^{ν_p} = p_d;
    update pressure dependent properties: b = b(p^{ν_p});
    calculate fine-scale total velocity u_T from p_d and p_v;
    /* inner loop */
    while (saturation equation not converged)
        solve linearized transport equation for S^{ν_s+1};
        ν_s = ν_s + 1;
        update saturation dependent properties:
        ⇒ λ = λ(S^{ν_s});
    end
end
n = n + 1
```

Fig. 3—The pseudo code of OBMM with SFI scheme for one time step

structed by

$$\mathbf{p}_d = \mathcal{P}\mathbf{p}_c. \quad \ldots\ldots\ldots\ldots\ldots\ldots\ldots\ldots\ldots\ldots \quad (22)$$

The fine-scale velocity calculated using $\mathbf{p}_d$ may be discontinuous across the interfaces of dual coarse blocks, since the basis functions assure flux continuity only in the interior of each dual block. To obtain a conservative fine-scale velocity, we solve the fine-scale Eq.2 locally for each primal coarse block with flux boundary conditions. The flux boundary conditions are obtained from $\mathbf{p}_d$. The fine-scale pressure computed in this manner is the primal fine-scale pressure, which we denote as $\mathbf{p}_v$. Then, the fine-scale velocity in the interior of primal coarse blocks is calculated from $\mathbf{p}_v$, while the velocity on the boundary of a primal coarse block is calculated from $\mathbf{p}_d$. Compressibility is taken into account in the fine-scale fluxes naturally when the fine-scale pressure is available.

Coupling Flow and Transport.. We choose the sequential fully implicit (SFI) algorithm to solve the coupled flow and transport equations. For each time step, in an outer loop we solve for the fine-scale pressure using OBMM and calculate the fine-scale total velocity, $\mathbf{u}_T$; in an inner loop we solve for the fine scale saturation implicitly according to Eq.5. The pseudo code for one time step is listed in Fig.3, where n denotes a time step and ν denotes the iteration level.

Note that for the finite-volume based OBMM, the restriction operator need to be constructed once as shown by Eq.17. Also note that when solving the saturation equations in the inner loops, the total velocity $\mathbf{u}_T$ is fixed.

Adaptive Updating of Basis Functions. The OBMM would not be efficient if we have to update the basis functions every iteration by solving Eq.7. Jenny *et al.* (2004, 2006) proposed adaptive updating of the basis functions according to the change of total mobility. However, as can be seen from Eq.7, the basis functions rely not only on the mobility, but also on pressure in compressible flows. Our adaptive updating of basis functions is performed as follows. If the condition

$$\frac{1}{1+\varepsilon_\lambda} < \frac{(\sum_l b_l\lambda_l)^\nu}{(\sum_l b_l\lambda_l)^*} < 1+\varepsilon_\lambda \quad \ldots\ldots\ldots\ldots\ldots\ldots \quad (23)$$

is not satisfied for all fine cells inside a dual coarse block, then the basis functions associated with that dual block should be recomputed. The superscript * here denotes the state in the last basis function update. The parameter ε_λ is a user defined adaptivity threshold. Usually, $0.1 \le \varepsilon_\lambda \le 0.2$ yields results close to those without adaptivity. Note that Eq.23 does not contain the absolute permeability, which is usually static.

Numerical Results

1D Compressible Single Phase Flow. First, we consider 1D single phase gas flow in a homogeneous permeability field. The purpose is to examine the accuracy of OBMM for compressible problems compared with other approaches.

The fluid is taken to be ideal gas and thus the PVT relation is simply

$$b = \frac{p}{p_0}, \quad \ldots\ldots\ldots\ldots\ldots\ldots\ldots\ldots\ldots\ldots \quad (24)$$

where p_0 is pressure at standard condition. The fine grid contains 100 fine cells and coarse grid has 5 blocks. The permeability is assumed to be constant. Initial pressure is constant at 1 atm. The left and right boundaries are kept at constant pressure, 10 and 1 atm, respectively. We define a dimensionless characteristic time τ as

$$\tau = \frac{\mu\phi L^2}{k(p_l - p_r)}. \quad \ldots\ldots\ldots\ldots\ldots\ldots\ldots\ldots\ldots\ldots \quad (25)$$

We compare the pressure results of OBMM with the FSA model as well as fine-scale reference solutions. Note that in the FSA model, we use the basis functions used by Lunati and Jenny (2005), which only depend on the total mobility. The basis functions in OBMM are computed from Eq.7.

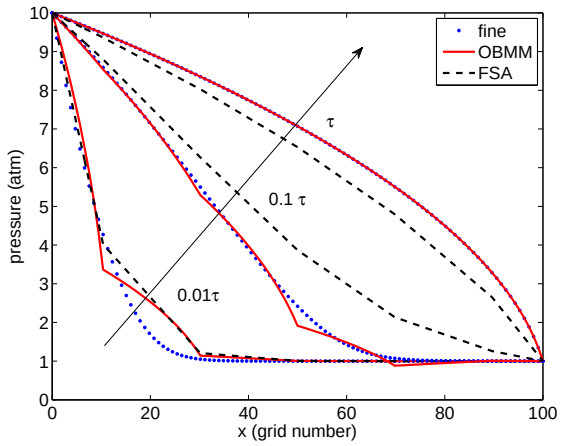

Fig. 4—Comparison of pressure results of OBMM, FSA and fine-scale reference solution for 1D single phase gas flow at several time steps.

OBMM shows some error at early time, which is mainly due to the fact that the elliptic basis functions do not capture the fine scale pressure distribution in the early transient period. OBMM quickly approaches the fine-scale reference solution at later time. At $t = \tau$, the results are exactly the same as the fine-scale solution. On the other hand, the FSA model shows somewhat larger errors at later time, which are mainly due to two reasons. One is the diagonal approximation of the coarse scale accumulation; the other is due to computing the basis functions without dependency on pressure (or b), which gives linear basis functions in this homogeneous single phase problem.

2D two-phase depletion problem. We now study two-dimensional two-phase flow. The permeability field is extracted from the top layer of the SPE 10 model (Christie and Blunt 2001). The variance of the logarithmic permeability of this model is $\sigma^2_{lnk} = 5.45$ as

shown in Fig.5, which is highly heterogeneous. The fine-scale grid contains 220×60 cells, and the coarse-scale grid contains 20×6 blocks. The upscaling factor is 110 (11×10).

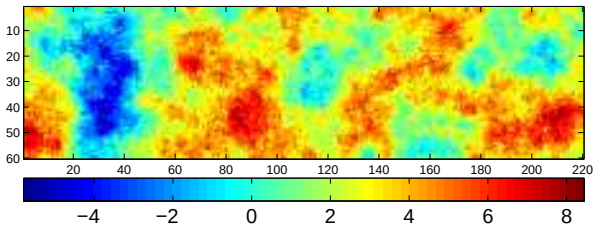

Fig. 5—Log-permeability of the top layer of the SPE 10 model

We study the depletion problem of oil and gas. The PVT properties are represented by formation volume factors as

$$\begin{aligned} b_g &= \frac{p}{p_0}, \\ b_o &= 1+10^{-3}(p-p_0). \end{aligned} \quad \ldots\ldots\ldots\ldots\ldots\ldots \quad (26)$$

Quadratic relative permeability curves are used. The viscosities of the two phases are $\mu_g = 1.8 \times 10^{-2}, \mu_o = 1$. The porosity is constant at 0.1. The field has an initial oil saturation of 0.5 and an initial pressure of 147 psi. The left boundary is kept at a constant pressure of 147 psi with $S_o = 0.5$, while the right boundary is brought to a constant pressure of 14.7 psi. Due to the pressure drop and compressibility differences, the gas expands faster than the oil, which causes the saturation change in the field.

We show a comparison of the OBMM solution with a fine-scale reference solution for the pressure and saturation fields at three time steps: $5^{-3}\tau$, 0.2τ and τ, where the dimensionless characteristic time is defined by

$$\tau = \frac{\mu_o \phi L_x^2}{\bar{k}(p_l - p_r)}. \quad \ldots\ldots\ldots\ldots\ldots\ldots\ldots\ldots \quad (27)$$

Here $\bar{k}$ is the median permeability. The time step is $5 \times 10^{-3}\tau$ for the first 10 time steps and then kept constant at 0.01τ thereafter. The adaptivity threshold ε in Eq.23 is 0.2.

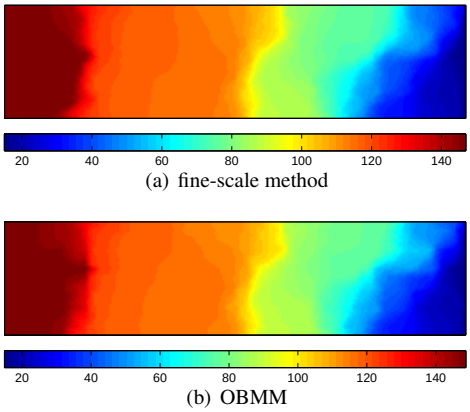

Fig. 6—Fine-scale pressure at $t = 5^{-3}\tau$: (a) using fine-scale method; (b) using OBMM

For all time steps, good agreement between OBMM and the fine-scale reference solutions is observed. We also report in Table 2 the error statistics and the cumulative percentage of basis functions that are recomputed. The pressure error, ε_p, and the saturation error, ε_s, are defined as

$$\begin{aligned} \varepsilon_p &= \frac{\|p^{ms} - p^f\|_2}{\|p^f\|_2}, \\ \varepsilon_s &= \|S^{ms} - S^f\|_2, \end{aligned} \quad \ldots\ldots\ldots\ldots\ldots\ldots \quad (28)$$

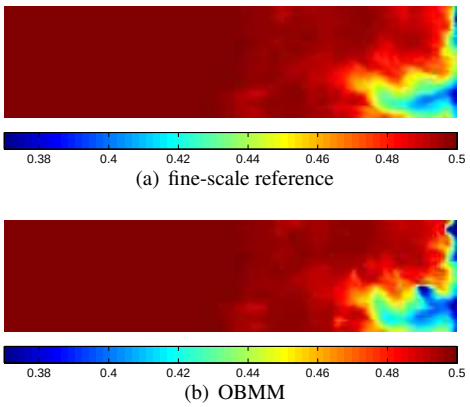

Fig. 7—Fine-scale oil saturation at $t = 5^{-3}\tau$: (a) using fine-scale method; (b) using OBMM

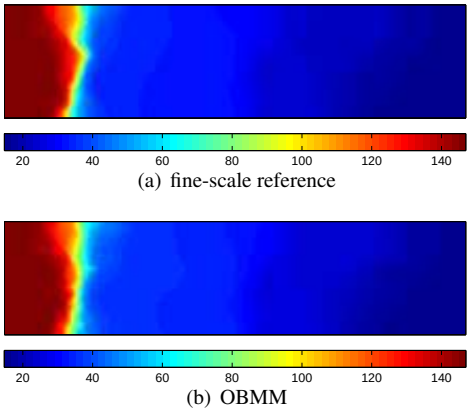

Fig. 8—Fine-scale pressure at $t = 0.2\tau$: (a) using fine-scale method; (b) using OBMM

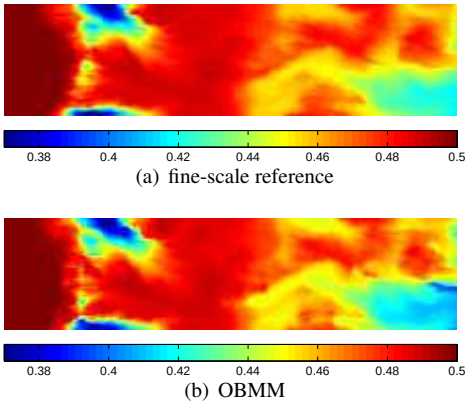

Fig. 9—Fine-scale oil saturation at $t = 0.2\tau$: (a) using fine-scale method; (b) using OBMM

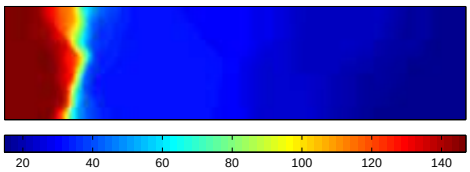

(a) fine-scale reference

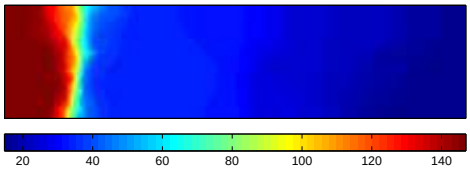

(b) OBMM

Fig. 10—Fine-scale pressure at $t = 1\tau$: (a) using fine-scale method; (b) using OBMM

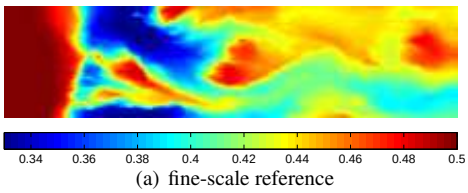

(a) fine-scale reference

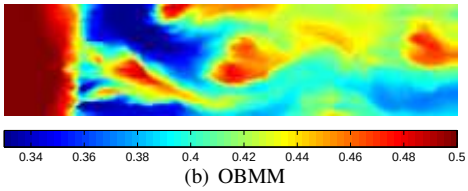

(b) OBMM

Fig. 11—Fine-scale oil saturation at $t = 1\tau$: (a) using fine-scale method; (b) using OBMM

t (PVI)	e_p	e_s	$f_p(\%)$
5e-3	1.13e-2	5.32e-5	12.22
0.2	1.80e-2	6.32e-5	7.96
0.8	1.64e-2	1.13e-4	8.79
1	1.62e-2	1.23e-4	7.98
1.5	1.64e-2	1.36e-4	6.50

Table 2—Errors and percentage of the recomputed basis functions for several times

where superscript f and ms, denote, respectively, the reference and OBMM solutions. The cumulative percentage of basis function updating f_p is the actual total number of updating basis functions from time zero to the current time divided by the total number without adaptivity.

Conclusions

An operator based multiscale method (OBMM) was developed. OBMM serves as a general algebraic multiscale framework. The prolongation operator is assembled from the basis functions. The restriction operator depends on the chosen discretization scheme. We have shown the restriction operators based on a finite volume method (FVM).

For the incompressible flow problem, the coarse-scale operator constructed by the finite-volume-based OBMM is identical to the MsFVM. Moreover, OBMM accounts for compressibility effects in a natural way. The fine-scale equations contain the fine-scale compressibility information, and the basis functions are calculated with compressibility effects. The coarse-scale operators constructed by OBMM account for compressibility by summing all the fine-scale information in a coarse block and distributing the contribution to the coarse nodes according to the basis functions.

For coupled flow and transport problems, a conservative fine-scale velocity field is crucial. A conservative velocity field is reconstructed by solving Neumman problems locally on the primal coarse blocks. A sequential fully implicit scheme is used to solve the coupled equations.

Test cases for compressible flow were presented, and the results obtained by OBMM are in very good agreement with fine-scale reference solutions. The permeability field in the test cases is highly heterogeneous, the compressibility is high, and the pressure variation is very large. Such challenging features show that OBMM is capable of solving highly compressible and strongly heterogeneous problems.

The efficiency of OBMM relative to standard fine-scale methods lies in the fact that we do not solve a global fine-scale system. Constructing and solving the coarse-scale equations takes little computational effort compared with solving the global fine-scale system. Adaptive updating of the basis functions can lead to great efficiency gains. OBMM is readily extendible to more complicated physics. Moreover, it does not depend on explicit description of grid geometry and can be directly applied to unstructured models. OBMM is purely algebraic and makes full use of the fine-scale properties and equations. Thus, OBMM can be implemented in existing reservoir simulators relatively easily. Compared with building a multiscale simulator from scratch, that will save a great deal of effort.

Nomenclature

$\mathcal{P}$	prolongation operator
$\mathcal{R}$	restriction operator
$\mathbf{C}_f$	fine-scale compressibility matrix
$\mathbf{C}_c$	coarse-scale compressibility matrix
$\mathbf{T}_f$	fine-scale transmissibility matrix
$\mathbf{T}_c$	coarse-scale transmissibility matrix
$\mathbf{p}_f$	fine-scale pressure vector
$\mathbf{p}_c$	coarse-scale pressure vector
ϕ_A^i	basis function in dual coarse block A for node i
$\mathbf{u}_T$	fine-scale total velocity
$\boldsymbol{x}$	coordinate
λ	mobility
b	inverse of formation-volume factor, $1/B$
l	phase indicator
k	global index of a fine node
K	global index of a coarse node
i, j	local index of a vertex of a dual coarse block
n	total number of fine nodes
N	total number of coarse nodes
Ω	entire physical domain
Ω_k	the fine cell centered on node k
Ω_K	the primal coarse block centered on coarse node K
$\tilde{\Omega}_A$	a dual coarse block

Acknowledgment

The authors gratefully acknowledge financial support from DOE grant DE-FG02-06-ER25727 and the Global Climate and Energy Project (GCEP) at Stanford University.

References

Aarnes, J. 2004. On the use of a mixed multiscale finite element method for greater flexibility and increased speed or improved accuracy in reservoir simulation. *Multiscale Modeling and Simulation*, **2**: 421–439.

Arbogast, T. 2002. Implementation of a Locally Conservative Numerical Subgrid Upscaling Scheme for Two-Phase Darcy Flow. *Computational Geosciences*, **6**: 453–481.

Arbogast, T. and Bryant, S. L. 2002. A Two-Scale Numerical Subgrid Technique for Waterflood Simulations. *SPE Journal*, **7**: 446–457.

Chen, Y., Durlofsky, L. J., Gerritsen, M., and Wen, X. H. 2003. A Coupled Local-Global Upscaling Approach for Simulating Flow in Highly Heterogeneous Formations. *Advances in Water Resources*, **26**: 1041–1060.

Chen, Z. and Hou, T. 2003. A mixed finite element method for elliptic problems with rapidly oscillating coefficients. *Mathematic Computation*, **72**: 541–576.

Christie, M. A. and Blunt, M. J. 2001. Tenth SPE comparative solution project: A comparision of upscaling techniques.. *SPE Reservoir Eval. & Eng.*, **4**: 308–317.

Hou, T. and Wu, X. H. 1997. A multiscale finite element method for elliptic problems in composite matrials and porous meida. *Journal of Computational Physics*, **134**: 169–189.

Jenny, P., Lee, S. H., and Tchelepi, H. A. 2003. Multiscale finite-volume method for elliptic problems in subsurface flow simulation. *Journal of Computational Physics*, **187**: 47–67.

Jenny, P., Lee, S. H., and Tchelepi, H. A. 2004. Adaptive Multiscale finite-volume method for multiphase flow and transportaion in porous media. *Mulitscale Modeling and Simulation*, **3**: 50–64.

Jenny, P., Lee, S. H., and Tchelepi, H. A. 2006. Adaptive fully implicit multiscale finite-volume method for multiphase flow and transport in heterogeneous porous media. *Journal of Computational Physics*, **217**: 627–641.

Lunati, I. and Jenny, P. 2005. Multiscale finite-volume method for Compressible Multiphase Flow in Porous Meida. *Journal of Computational Physics*, **216**: 616–636.

Tchelepi, H. A., Jenny, P., Lee, S. H., and Wolfsteiner, C. 2007. Adaptive Multiscale Finite Volume Framework for Reservoir Simulation. *SPE Journal*, **12**: 188–195.

Zhou, H. 2006. Operator Based Multiscale Method for Compressible Flow. Master's thesis, Stanford University (2006).

Hui Zhou is a PhD student of in the Department of Energy Resources Engineering at Stanford U. **Hamdi A. Tchelepi** is Associate Professor of Energy Resources Engineering at Stanford U. email:tchelepi@stanford.edu